Eur. Phys. J. D **17**, 255–259 (2001)

**THE EUROPEAN PHYSICAL JOURNAL D**

EDP Sciences


# Constrained order in frustrated 2D optical patterns

S. Residori[a] and N. Olivi-Tran

I.N.L.N.[b], Université de Nice Sophia Antipolis, 1361 route des Lucioles, 06560 Valbonne, France

Received 19 January 2001 and Received in final form 2 June 2001

**Abstract.** In 2D optical patterns obtained in a Liquid Crystal Light Valve with optical feedback, we show a new kind of geometrical frustration which comes from the imposed form of the boundaries. The circular section of the incoming laser beam presents a symmetry which belongs to the O(2) group, whereas the optical feedback selects patterns with a symmetry restrained to a dihedral subgroup of O(2). By imposing boundaries which respect the symmetry of the dihedral group, we lift the frustration and obtain perfectly ordered patterns.

**PACS.** 42.79.Kr Display devices, liquid-crystal devices – 42.65.Pc Optical bistability, multistability, and switching – 61.44.Br Quasicrystals

## 1 Introduction

Geometrical frustration is a subject of great interest up to now [1,2]. In particular, it can play a role in nonlinear pattern forming systems. For example, geometrical frustration may arise whenever the shape of the boundary has a symmetry which is not commensurate with the one of the patterns. Here we show that this kind of frustration may be removed or controlled by adjusting the shape of the boundary in order to accommodate the symmetry of the patterns. The experiment is performed on 2D optical patterns obtained in a Liquid Crystal Light Valve (LCLV) with nonlocal feedback, as originally introduced in reference [3]. This system is well-known for studying pattern formation. Many different dynamical behaviors were observed, depending both on the geometrical construction of the optical feedback loop and on the physical parameters of the liquid crystals [4].

It is well-known that boundary conditions influence the dynamics of nonlinear pattern forming systems both by altering the symmetry of the spatial structure and through the restriction they introduce in the parameter space. Besides these effects, a pinning mechanism occurs, which constrains the pattern to choose a specific direction with respect to the boundary. For example, it has been shown in Rayleigh-Benard convection [5] that rolls tend to align perpendicularly to the sidewalls of the fluid container, giving rise to a curvature effect which is responsible for the time dependence of the observed patterns. Another clear evidence of geometrical frustration may be found in a magnetic foam experiment [6] where the insertion of a circular obstacle leads to a strong modification of the cellular arrangement. Also, the hexagon-square transitions observed in ferrofluids [7] and in Marangoni convection [8] manifest themselves by the pinning of the secondary structure both to the defects of the hexagonal structures and to the borders of the system. Then, quasicrystalline patterns are observed in Faraday waves experiment, where geometrical frustration comes from the confinement of the fluid [9]. Of a different nature are the quasi-patterns observed in Faraday experiment with a high viscosity fluid, where the simultaneous forcing with two frequencies leads to bicriticality in the wavenumber space [10]. In this case, dissipation rules out all the linear modes of the container, and frustration is due to the simultaneous excitation of nonlinear modes with incommensurate wavenumbers.

Recently, geometrical frustration has also been proposed [11] as a possible explanation for the complex spatio-temporal dynamics observed in a Liquid Crystal Light Valve (LCLV) with feedback. In this case, frustration arises from the competition between the geometrical constraints (structure of the optical cavity, rotation of the feedback image) and the physical constraints (light-matter interaction). Again, the presence of several modes with incommensurate wavenumbers leads to quasi-crystals or to pattern competition [12].

Another kind of geometrical frustration which naturally appears in optics, is associated to the size and shape of the pumping light beam. As shown in reference [13], restrictions on the system size may greatly change the geometrical repartition of patterns. Indeed, when the profile of the laser beam is smaller than the basic size of the transverse spatial structure, a change of the symmetry of the patterns is observed. Several experimental verifications have been reported [14]. This kind of frustration comes from the strong limitation of the size of the system, which results in strong deformations of the basic structure. For example, if an hexagon cannot fit inside the available

[a] e-mail: `residori@inln.cnrs.fr`
[b] UMR 6618 du CNRS

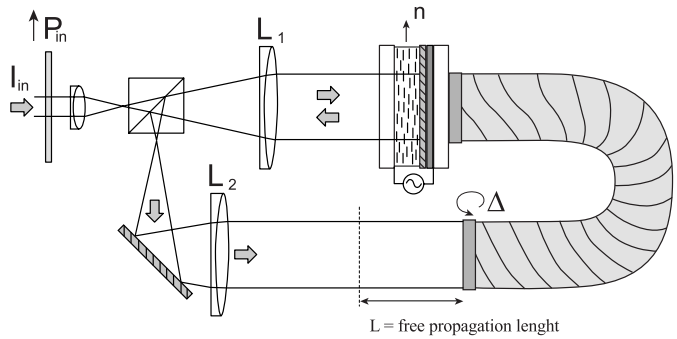


**Fig. 1.** Experimental setup: the two confocal lenses $L_1$ and $L_2$ provide a 1:1 image-forming system from the front side of the LCLV to its rear side. The optical feedback loop is closed by a fiber bundle, which can be twisted in order to provide a rotation angle $\Delta$. $P_{\rm in}$ is a polarizer selecting the input light polarization. Its orientation is vertical as well as the liquid crystal director **n**.

space, it may loose one cell and transform into a pentagon, which corresponds to a drastic change of symmetry.

Here we want to study the geometrical frustration which is related more to the shape of the boundaries than to their size. Therefore, we will restrict ourselves to the case where the size of the system is large enough compared to the basic length of the patterns. In this case, geometrical frustration is introduced by the circular profile of the optical beam. Actually, the Gaussian profile of the illumination forces the system to be invariant under rotations and reflections in the transverse plane (O(2) symmetry group). This group of symmetry, respected by any circular boundary, does not fix any of the dihedral subgroups naturally selected by the dynamics of the system [4]. But, since boundaries introduce a correlation length over which patterns are pinned, depending on the mutual size of the boundaries and of the pinning length, the overall symmetry of the patterns can be affected by the shape of the boundaries.

In Section 2, we present the experimental setup and the basic features of the pattern formation process in the LCLV with feedback. The experimental results are presented in Section 3, where we show that geometrical frustration may also induce dynamics of patterns. Besides, we show that the frustration can be removed through the application of boundaries which respect the dihedral symmetry of the basic structure. We present our numerical approach for analyzing the patterns and we discuss the results in Section 4. Our processing allows us to evaluate the correlation length for the pinning mechanism, which can be an useful indication for determining the border between small and large systems, a problem which often occurs in the realization of experimental systems.

## 2 Experimental setup

A schematic of the experimental setup is displayed in Figure 1. The LCLV is essentially a mirror sandwiched between a nematic liquid crystal and a photo-conductive layer. An AC voltage is applied between the photo-conductor and the liquid crystal. In the presence of light on the photo-conductor, the voltage drop across the liquid crystal layer increases inducing a reorientation of the LC molecules. For the reflected light, this reorientation produces a phase change. Transverse patterns in the optical field are due to diffraction which converts the phase modulation, generated within the LCLV, into amplitude modulation. This latter one, on its turn, modifies the properties of the LCLV. In this way, a positive feedback is realized for all those spatial frequencies satisfying the resonance conditions $q^2L/2k = \pi/2, 3\pi/2, ...$, where $q$ is the field transverse wavenumber, $k = 2\pi/\lambda$ is the optical wavenumber and $L$ is the free propagation length [15]. In our case $\lambda = 632$ nm is the wavelength of an He–Ne laser and $L$ can vary between 20 and 60 cm. The laser beam is expanded up to a diameter of 2.5 cm which is the transverse size of the LCLV. By inserting a circular diaphragm of 1 cm diameter in front of the LCLV, only a central region is let to be active so that the medium is uniformly illuminated. Indeed, the intensity profile of the laser beam can be considered flat on its central region and it is not playing any role in the stability of the observed patterns.

The natural symmetry of the transverse patterns here arising is the hexagonal one, due to the quadratic character of the light-matter interaction [16]. The characteristic size of the pattern is the one satisfying the resonance condition $q^{-1} \simeq (\lambda L)^{-1/2}$, *i.e.*, of the order of a few tenth of mm for the parameters currently set in the experiments.

The feedback is realized by means of a coherent optical fiber bundle. By twisting the bundle, the image on the back of the LCLV can be rotated by any angle $\Delta = 2\pi/N$ with respect to the front image. This rotation impose an overall $N$-fold symmetry which can or not be consistent with the symmetry provided by the quadratic nonlinearity of the light-medium interaction. In the present experiment, we fix the rotation order to $N = 3$ or $N = 4$, values which satisfy the quadratic nature of the physical interactions. Therefore, rotation does not introduce any geometrical frustration [11] and we expect patterns to be ordered crystals. But, because of the circular shape of the transverse boundary geometrical frustration does indeed appear. Close to the boundaries the pattern is distorted and composed by distinct spatial domains with different orientation of the basic structure. By imposing boundaries with a shape which belongs to the same dihedral group of the basic symmetry, the pattern is pinned in a single direction over its entire extension and frustration is thus removed.

## 3 Results and numerical analysis

We show in Figure 2a a typical pattern observed for $N = 3$. While in the center there is an almost perfect tiling of hexagons, close to the borders the regular arrangement is becoming loose and the pattern is composed of domains tiled with hexagons oriented in different directions. In the course of time, these domains are sliding and reorienting,

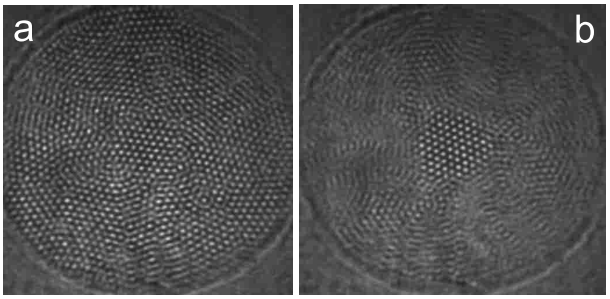


**Fig. 2.** (a) A typical pattern obtained for a rotation order $N = 3$ and with circular boundary; (b) for the same conditions, time average of successive images.

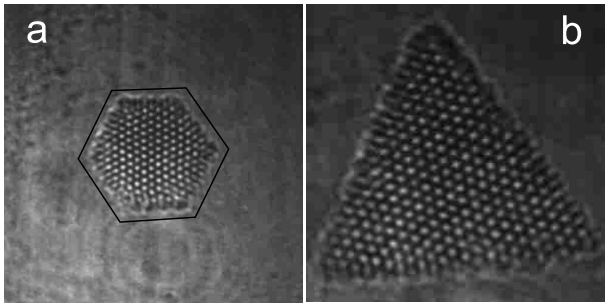


**Fig. 3.** Effect of boundary for $N = 3$: (a) a single domain pattern obtained through the application of a hexagonally shaped boundary; (b) a single domain pattern obtained through the application of a large triangular boundary.

thus giving rise to slow dynamics. In Figure 2b we show a pattern resulting from the time average of successive images over 5 s. It can be noticed that the hexagons in the center remain fixed and ordered while towards the borders the averaged image is characterized by much less contrast. This is a signature of the fact that in these locations the pattern is moving and changing. In this case, we should recover the symmetry of boundaries, as originally predicted and observed in Faraday waves experiments [17]. This effect has also been observed in Rayleigh-Benard experiment [18] and in an optical photorefractive oscillator [19]. In our case, time average results in portions of rolls parallel to the boundaries, which is in agreement with the previous observations.

Notice that, with no feedback rotation, we obtain the same results as in the case of $N = 3$ rotation order. However, without image rotation, the systems becomes more sensitive to LCLV inhomogeneities and to optical misalignments. Since we want to avoid any other source of pattern pinning than boundaries, we prefer to work with feedback rotation.

In order to impose boundaries which correspond to the rotation order $N = 3$, we insert in the optical loop a diaphragm with an hexagonal and triangular shape. As it can be seen in Figures 3a and 3b, inside the boundaries the resulting pattern is almost perfectly ordered, like a single-domain 2D crystal. We used here two types of boundaries: a small hexagon and a large triangle. The fact that both present ordered patterns is a proof that the boundary size has no effect as long as it respects the underlying symmetry.

We repeat the same experience for $N = 4$ and we show the result in Figure 4. Figure 4a is the center of a typical pattern observed for a circular boundary. Again, the center is tiled with an almost ordered square pattern while the outer regions show defects and slow dynamics. In Figures 4b–4d we impose a small square boundary. A slight distortion of the square boundary is responsible for the apparition of a dislocation, as it is shown in Figure 4b. In Figure 4c we show that a small re-alignment of the boundary can improve the pinning of the square pattern, so that the dislocation relaxes and vanishes. A perfectly ordered and single-domain square pattern is shown in Figure 4d, for an almost perfect square boundary. For the sake of completeness, we show in Figures 4e and 4f the patterns

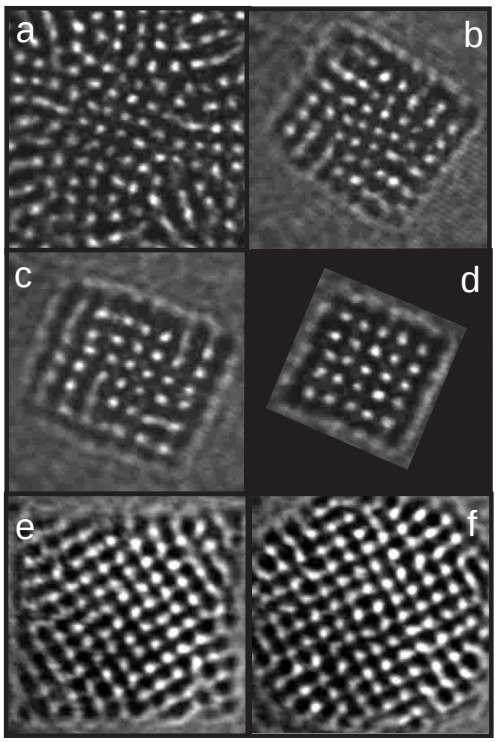


**Fig. 4.** Effect of boundary for $N = 4$: (a) circular boundary; (b) application of a slightly distorted square boundary induces the creation of a dislocation; (c) a small re-alignment of the boundary improves the pinning so that the dislocation relaxes and disappears; (d) a single domain pattern fixed by the application of a perfect square; (e) ordered pattern resulting through the application of a large square and (f) through the application of an octagonally shaped boundary.

obtained for a large square and a large octagon, respectively. We can notice that they are both highly ordered.

In order to analyze the patterns, we process the images by imposing an intensity threshold and then performing a binarization. This way, we are able to obtain the location of each cell composing the patterns. On the binarized images, we determine numerically the angle between three neighboring cells. Especially for disordered patterns, we have to introduce a tolerance for the distance between nearest neighbors. Image sizes ranges from $150 \times 150$ to

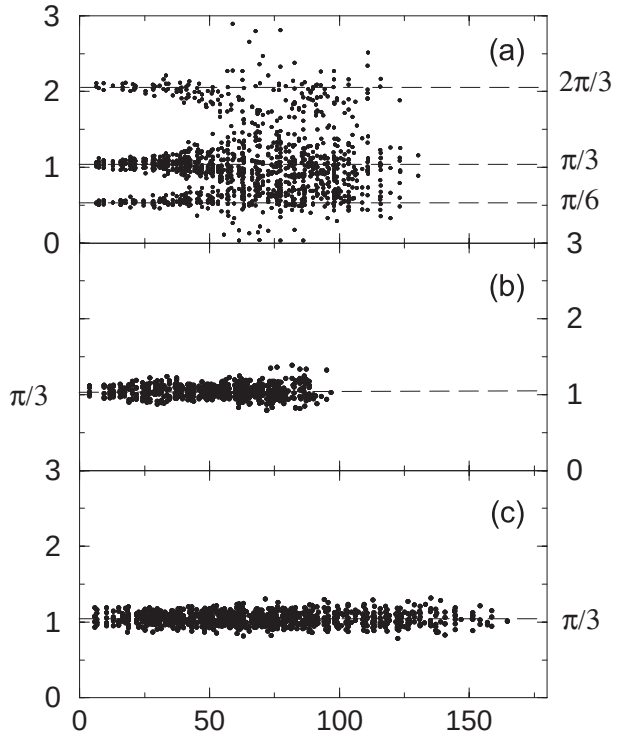


**Fig. 5.** Angles (measured in radians) between three neighboring cells as a function of the distance from the center of the LCLV and for $N = 3$: (a) circular boundary; (b) hexagonally shaped boundary and (c) larger and triangular boundary.

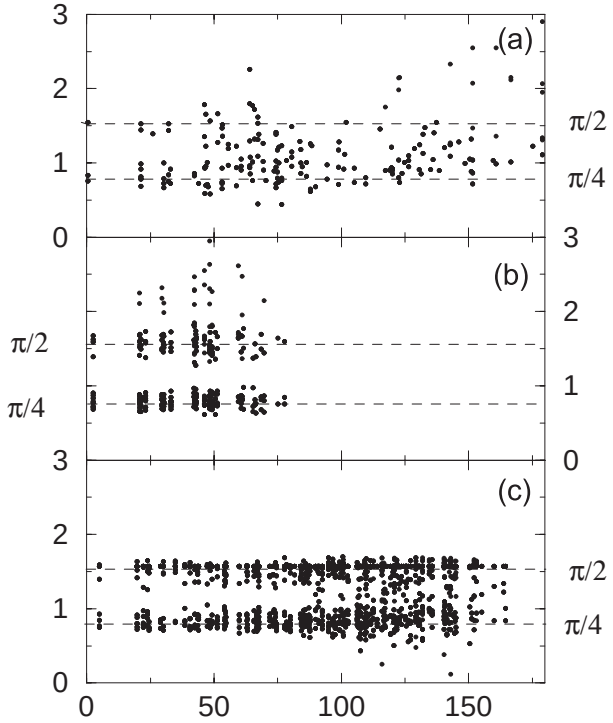


**Fig. 6.** Angles (measured in radians) between three neighboring cells as a function of the distance from the center of the LCLV and for $N = 4$. (a) circular boundaries; (b) square boundary and (c) larger and octagonal boundary.

$200 \times 200$ pixels. For the hexagonal patterns, the average distance between 2 neighboring cells is found to have a value of $10 \pm 2$ pixels, corresponding to the average cell distance and tolerance, respectively. In real units, this distance corresponds to 500 $\mu$m, approximatively. For the square patterns, the corresponding average cell distance is multiplied by a factor $\sqrt{3}$, in agreement with the linear analysis which predicts a larger length scale for the patterns characterized by an even rotation order [11].

In Figures 5 and 6 we report the angles between three neighboring cells as a function of the distance from the center of the image (that we assume to coincide with the center of the LCLV), for $N = 3$ and 4, respectively. Figure 5a is obtained for a circular boundary and in the case $N = 3$. Figures 5b and 5c correspond to the angular analysis of Figures 3a and 3b, respectively. Figure 6a is obtained for a circular boundary and in the case $N = 4$. Figures 6b and 6c correspond to the angular analysis of Figures 4d and 4f, respectively.

## 4 Discussion

The angle analysis allows the quantification of the pinning length introduced by the boundaries onto the pattern. For circular boundaries, disorder is located over an annular region starting at the boundaries. The width of this annular region corresponds to the pinning length. When we introduce boundaries which respect the underlying symmetry, the extension of the pinned region cover the whole pattern.

Indeed, from Figures 5a and 6a, corresponding to $N = 4$ and 3, respectively, it becomes clear that patterns are ordered over a distance which is approximatively equal to 50 pixels from the center of the circle. The transition to the disorder is identified by the disappearance of the band structure in the distributions of points. Then, we can conclude that geometrical frustration is induced by the circular shape of the boundaries over a correlation length which stops at approximatively 50 pixels from the center. In other words, the center of the images with circular boundaries remains ordered over a disk which has a radius approximately three and five times larger than the typical cell distance for the square and the hexagonal pattern, respectively.

Moreover, by varying the aperture size in the case of a circular shape, we observe that the pinning length remains the same as long as the system size is large enough with respect to the width of the central ordered region. Then, we can notice that close to the center the angles separate in 3 or 2 values, $2\pi/3$, $\pi/3$ and $\pi/6$ for Figure 5a, and $\pi/2$ and $\pi/4$ for Figure 6a, respectively. This is the signature of the fact that some cells in the pattern are missing. As a consequence, the basic symmetry is locally lowered which results in the calculation of angles which are multiples or sub-multiples of the feedback rotation angle.

As it can be seen in Figures 6b and 6c, for the square case the two angles $\pi/2$ and $\pi/4$ are present also when we

impose a square boundary. While the first of these two values reflects the basic square symmetry and remains constant all over the pattern extension, the second value is a consequence of the tolerance introduced in the calculation of the distance. Indeed, this value comes from taking into account the diagonals of the squares, which is difficult to avoid with our tolerance in the distances. Given the same tolerance, the geometry itself removes this problem for the hexagons. In this case, as it is shown in Figures 5b and 5c, we obtain a single value $\pi/3$ for all the calculated angles, corresponding to a perfect 2D crystal.

An easy comparison between Figures 5b and 5c on one hand, and between Figures 6b and 6c on the other hand, shows that a larger pinned and ordered pattern can be obtained by simply enlarging the size of the boundary.

## 5 Conclusion

In conclusion, we have shown that geometrical frustration can arise because of the circular shape of the boundaries, when a lower symmetry is selected for the basic pattern. This frustration can be removed by the application of boundaries which reinforce the basic symmetry of the patterns. The fundamental mechanism is a pinning of the basic structure in a single direction of orientation, which renders the whole pattern fully correlated over one single domain. By means of a numerical analysis, we have shown that the pinning introduced by the boundaries changes with the shape of the container. This pinning length is an important scale for the pattern formation problem, since it defines the border between the small and large aspect systems, where for a large system it is usually intended a system not affected by the boundary conditions.

We are grateful to F. Graner for stimulating this article. This work has been financially supported by the *Action Concertée Incitative Jeunes* of the French Ministry of Research.

## References

1. M.C. Escher, *The Graphic Work of M.C. Escher* (Ballantine Books, New-York, 1971).
2. J.F. Sadoc, R. Mosseri, *Frustration géométrique* (Édition Eyrolles, Paris, 1997).
3. S.A. Akhmanov, M.A. Vorontsov, V.Y. Ivanov, A.V. Larichev, N.I. Zheleznykh, J. Opt. Soc. Am. B **9**, 78 (1992).
4. See *e.g.* special issue *Pattern formation in nonlinear optical systems*, edited by R. Neubecker, T. Tschudi, Chaos, Solitons & Fractals **10**, (1999); F.T. Arecchi, S. Boccaletti, S. Ducci, E. Pampaloni, P.L. Ramazza, S. Residori, J. Nonlin. Opt. Phys. Mat. **9**, 183 (2000).
5. G. Ahlers, D.S. Cannell, V. Steinberg, Phys. Rev. Lett. **54**, 1373 (1995).
6. F. Graner, Y. Jiang, E. Janiaud, C. Flamant, Phys. Rev. E **63**, 011402 (2000).
7. B. Abou, J.E. Weisfreid, S. Roux, J. Fluid Mech. **416**, 217 (2000).
8. K. Nitschke, A. Thess, Phys. Rev. E **52**, R5772 (1995); M.F. Schatz, S.J. van Hooke, W.D. McCormick, J.B. Swift, H.L. Swinney, Phys. Fluids **11**, 2577 (1999).
9. B. Christiansen, P. Alstrom, M.T. Levinsen, Phys. Rev. Lett. **68**, 2157 (1992); R.A. Barrio, J.L. Aragon, C. Varea, M. Torres, I. Jimenez, F. Montero de Espinosa, Phys. Rev. E **56**, 4222 (1997).
10. W.S. Edwards, S. Fauve, Phys. Rev. E **47**, R788 (1993).
11. S. Residori, N. Olivi-Tran, E. Pampaloni, Eur. Phys. J. D **12**, 15 (2000).
12. E. Pampaloni, P.L. Ramazza, S. Residori, F.T. Arecchi, Phys. Rev. Lett. **74**, 259 (1995); S. Residori, P.L. Ramazza, E. Pampaloni, S. Boccaletti, F.T. Arecchi, Phys. Rev. Lett. **76**, 1063 (1996).
13. F. Papoff, G. D'Alessandro, G.-L.Oppo, W.J. Firth, Phys. Rev. A **48**, 634 (1993).
14. R. Macdonald, H. Danlewski, Opt. Commun. **113**, 111 (1994); E. Ciaramella, M. Tamburrini, E. Santamato, Phys. Rev. A **50**, R10 (1994); T. Ackemann, W. Lange, Phys. Rev. A **50**, R4468 (1994); E. Pampaloni, P.L. Ramazza, S. Residori, F.T. Arecchi, Europhys. Lett. **25**, 587 (1994).
15. W.H.F. Talbot, Philos. Mag. **9**, 401 (1836).
16. G. D'Alessandro, W.J. Firth, Phys. Rev. A **46**, 537 (1992); G. D'Alessandro, E. Pampaloni, P.L. Ramazza, S. Residori, F.T. Arecchi, Phys. Rev. A **52**, 4176 (1995).
17. B.J. Gluckman, P. Marcq, G. Bridger, J.P. Gollub, Phys. Rev. Lett. **71**, 2034 (1993).
18. L. Ning, Y. Hu, R.E. Ecke, G. Ahlers, Phys. Rev. Lett. **71**, 2216 (1993).
19. J. Farjas, D. Hennequin, D. Dangoisse, P. Glorieux, Phys. Rev. A **57**, 580 (1998).